Saudi Pharmaceutical Journal 32 (2024) 102125

HOSTED BY

Contents lists available at ScienceDirect

Saudi Pharmaceutical Journal

journal homepage: www.sciencedirect.com

Original article

Development of topical silver nano gel formulation of Bixin: Characterization, and evaluation of anticancer activity

Swapnil S. Patil [a], Preeti khulbe [a], Manojkumar M. Nitalikar [b], Kuntal Das [c], Mallikarjuna B.P. [d], Sultan Alshehri [e], Amro Mohammed Sawadi Khormi [f], Mutlaq Eidhah M. Almalki [g], Syed Arif Hussain [h], Syed Imam Rabbani [i], Syed Mohammed Basheeruddin Asdaq [j,*]

[a] Gyan Vihar School of Pharmacy, Suresh Gyan Vihar University Jaipur, 302017 Rajasthan, India
[b] Rajarambapu College of Pharmacy Kasegaon, 415404 Maharashtra, India
[c] Mallige College of Pharmacy, #71, Silvepura, Chikkabanavara Post, Bangalore 560090, India
[d] MB School of Pharmaceutical Sciences (Erstwhile Sree Vidyanikethan College of Pharmacy), Mohan Babu University, Tirupati, Andhra Pradesh, 517102, India
[e] Department of Pharmaceutics, College of Pharmacy, King Saud University, 11451 Riyadh, Saudi Arabia
[f] Department of Pharmacy, King Saud University Medical City, Riyadh, Saudi Arabia
[g] Department of Pharmaceutical Sciences, King Saud University, Riyadh 11451, Saudi Arabia
[h] Department of Respiratory Care, College of Applied Sciences, AlMaarefa University, Dariyah 13713, Riyadh, Saudi Arabia
[i] Department of Pharmacology and Toxicology, College of Pharmacy, Qassim University, 51452 Buraydah, Saudi Arabia
[j] Department of Pharmacy Practice, College of Pharmacy, AlMaarefa University, Ad Diriyah 13713, Saudi Arabia

ARTICLE INFO

Keywords:
Drug design
Bixin
Silver nanoparticles
Formulation
Characterization
Anticancer
Nanogel

ABSTRACT

Objective: Skin cancer refers to the pathological condition characterized by the proliferation of atypical skin cells in an uncontrolled manner. Plant-based products such as bixin although show promising anticancer properties, but maintaining their stability in a formulation is a difficult task. The objective of the research is to formulate a silver nanoparticle gel preparation of bixin and evaluate its anticancer properties.

Methods: The extract from *Bixa orellana* seed was prepared by hot extraction technique to isolate the active ingredient, bixin. A green synthesis approach was utilized for preparing the silver nanoparticle gel of bixin (BOAgNPs). Characterization of silver nanoparticles was done using FTIR, scanning electron microscopy, compatibility study, homogeneity testing, pH evaluation, and drug content determination. The *in-vitro* anticancer activity was performed using cell lines (B16F10) and *in-vivo* by chemical carcinogen (7,12-dimethylbenz (a) anthracene) in mice.

Results: The BOAgNPs-loaded topical gel was found to be homogeneous (clear orange color) and pH-compatible (pH ≈ 6.66) with the skin. The characterization studies indicated the presence of all functional groups in the formulation. An optimized batch of bixin-nano gel showed about 60% inhibitory effects on B16F10 cell lines (*in-vitro* activity) when equated with a reference drug, 5-fluorouracil. The *in-vivo* anticancer study suggested suppression of tumorigenesis and promotion of the healing process with bixin-nano gel application on the skin.

Conclusion: The results suggested the promising anticancer property of bixin when formulated in silver nanoparticle gel. The preparation of silver particles nano gel with bixin might provide an effective alternative option for treating skin cancers, provided more research complements the findings of the present study.

1. Introduction

The utilization of a novel drug delivery system is an innovative strategy in the field of drug administration, aiming to reduce the inherent constraints connected with routine drug delivery systems. In the coming years, there seems to be a rising recognition of the untapped

* Corresponding author at: Department of Pharmacy Practice, College of Pharmacy, AlMaarefa University, Dariyah, 13713 Riyadh, Saudi Arabia.
E-mail addresses: swapnil.patil0707@gmail.com (S.S. Patil), preeti.khulbe@mygyanvihar.com (P. khulbe), mmnitalikar@gmail.com (M.M. Nitalikar), drkkdsd@gmail.com (K. Das), mallibp@gmail.com (M. B.P.), Salshehri1@ksu.edu.sa (S. Alshehri), Amr1411@hotmail.com (A.M.S. Khormi), Malmalki3@ksu.edu.sa (M.E.M. Almalki), pulmoarif@gmail.com, pulmoarif@gmail.com (S.A. Hussain), syedrabbani09@yahoo.com (S.I. Rabbani), sasdag@um.edu.sa, sasdaq@gmail.com (S.M.B. Asdaq).

https://doi.org/10.1016/j.jsps.2024.102125
Received 22 April 2024; Accepted 1 June 2024
Available online 2 June 2024

potential of alternative systems for treating diseased conditions (Qiu et al., 2022). Nevertheless, the drug delivery technique employed for the administration of the herbal medicine to the patient is reported to be conventional and antiquated, leading to diminished effectiveness of the medication (Matalqah et al., 2020). The potential utilization of cutting-edge medication administration technology in the field of herbal medicine presents opportunities to improve efficacy and reduce side effects related to various herbal components and herbs (Khizar et al., 2023).

Skin cancer refers to the pathological condition characterized by the proliferation of atypical skin cells in an uncontrolled manner. The phenomenon is caused by untreated DNA damage in skin cells, which is mostly caused by UV radiation from sunshine. This damage can lead to mutations or genetic abnormalities, which can cause skin cells to proliferate quickly and produce malignant tumors. (Dildar et al., 2021). Skin cancers are reported to be the malignancies that are most commonly diagnosed in individuals of Caucasian descent globally. This prevalence is attributed to the escalating levels of exposure to ultraviolet (UV) radiation, which has led to a continuous rise in the incidence of these cancers (Dorrell and Strowd, 2019). Previous studies distinguished skin cancer to be an aberration in the regulation of apoptosis, resulting in either insufficient cell death or excessive cell proliferation and survival inside the epidermis (Ahmed et al., 2020). According to an analysis conducted across 185 countries, the total cost of treating such cancers is estimated to be trillions of dollars to the global economy (Bray et al., 2018).

The primary challenges associated with chemotherapeutic treatments encompass the occurrence of significant lateral effects and the progression of resistance to several drugs. Several mechanisms that contribute to the resistance of cancer cells to chemotherapy include drug efflux systems, intensification of drug targets, and alterations in drug kinetics (Gonçalves et al., 2021). In addition, there is a emergent curiosity in academia in the usage of complementary and alternative medicines, mostly driven by the drawbacks connected with standard cancer chemotherapies and the perceived benefits of employing more holistic therapy approaches (Youn et al., 2023).

The literature that is now accessible indicates that extracts from a wide variety of plant parts, such as roots, bulbs, barks, leaves, and stems, have shown a great deal of promise as anticancer medications or as starting materials for the creation of novel pharmaceuticals. (Huang et al., 2022). Traditional medicines frequently employ them in the custom of homemade tinctures, teas, or crude extracts. Several active constituents isolated from herbs such as *Curcuma longa, Fagonia indica, Garcinia olongifolia, Hedyotis diffusa, Morus alba, Perilla frutescens,* and *Tripterygium wilfordii* have been reported to possess anticancer properties (Cruz-Martins, 2023).

One of the primary challenges associated with natural products is the inherent variability in their production processes, which consequently leads to variations in their chemical makeup. This variability poses limitations in terms of determining and adjusting the appropriate dosage, as well as identifying the most acceptable route of administration (Jarouche et al., 2019). Among several methods, the creation of silver nanoparticle gel is said to be as easy as combining metal ions with reduced polyoxometalates, which has the dual effects of acting as a reducing and stabilizing agent. (Panahishokouh et al., 2023). Preparation of such formulation achieves optimum distribution of drug content, stability, texture, and particle size to produce the desired therapeutic effects. The technique is extensively studied in the literature and used for administering antimicrobial, anticancer, and anti-inflammatory medications (Mughees and Wajid, 2021). Some of the common herbal medicines reported to show optimal therapeutic acitivity when administered by silver nano particle forumulation are *Coriander sativum, Amaranthus gangeticus, Ocimum santum, Syzygium aromaticum, Origanum vulgare* and *Soymida febrifuga* (Panja et al., 2021)*Bixa Orellana* (Family: *Bixaceae*) is a tiny tree or shrub approximating 3 to 5 m in height and commonly grows in several regions of Asia, America, Europe, and East Africa. The plant features alternating leaves, brown bark, and regular, fragrant blooms with pyramid-shaped seeds.

(Coelho et al., 2022). The seeds have commercial value since they contain a pigment called bixin that is extensively employed as a natural tinting agent in the paint and food industry. Bixin ($C_{25}H_{30}O_4$) is an orange-red colored component containing mostly the carotenoids (80 %) (Shadisvaaran et al., 2023). Owing to the presence of carotenoids, this pigment has been shown to have a number of pharmacological properties, including the ability to reduce fibrosis, function as an antioxidant, reduce inflammation, lower blood cholesterol, treat diabetes, and reduce allergies (Tao et al., 2021).

Bixin has an anticancer activity against several types of cancer demonstrated on different cell lines including HL60 (leukemia), B16 (melanoma), U20S (osteosarcoma), PC3 (prostate), HCT-116 (colon), MCF (breast), and BHP-16 (papillary thyroid) (Ashraf et al., 2023). Nevertheless, there is scant evidence supporting bixin's role in nanoparticle gel formulation and on the skin cancer-causing B16F10 cell lines. Therefore, the current study was planned to design and formulate a silver nanoparticle gel preparation of bixin, characterize it, and evaluate the *in-vitro* as well as *in-vivo* anticancer properties in experimental models.

Table 1
Formulation table of BOAgNPs nanogel.

Ingredient	Batch					
	F1	F2	F3	F4	F5	F6
BOAgNPs (ml)	1.0	1.0	1.0	1.0	1.0	1.0
Carbapol (g)	0.5	1.0	1.5	–	–	–
HPMC K15 (g)	–	–	–	0.5	1.0	1.5
Propylene glycol (ml)	10	10	10	10	10	10
Triethanolamine (ml)	1.0	1.0	1.0	1.0	1.0	1.0
Methyl Paraben (g)	0.1	0.1	0.1	0.1	0.1	0.1
Propyl Paraben (g)	0.5	0.5	0.5	0.5	0.5	0.5
Water (ml)	q.s	q.s	q.s	q.s	q.s	q.s

Notes: The amount of drug and $AgNO_3$ per ml of the BOAgNPs were 0.15 gm and 0.000338 gm, respectively.

2. Material and methods

2.1. Drugs and reagents

The fresh and dried seeds of *Bixa orellana* were received from Sree Ratna Enterprises, Gokavaram, Andhra Pradesh, and were cultivated in the same region. The additional excipients and compounds were obtained from Sigma Aldrich (MH, India).

2.2. Extraction method

The seeds of *B. orellana* were subjected to two days of sunlight drying, followed by a further 72-hour duration in a tray dryer at a temperature of 50 °C. The powdered material required for the extraction process was obtained through the mechanical grinding of the dried *B. orellana* seed. 30 g dried powdered samples were taken in three soxhlet apparatus containing 200 ml of solvent. The extraction was carried out in a soxhlet apparatus for 12 hr with different solvents like methanol, ethanol, acetone, and hexane at 60 °C, 70 °C, 50 °C, and 60 °C respectively. All precautions were followed to maintain the integrity of the isolated Bixin as described in the literature (David et al., 2022).

2.3. Green synthesis of Bixa orellana silver nanoparticles (BOAgNPs)

The experiment was carried out with 20 ml of 0.2 mm, 1 mm and 2 mm $AgNO_3$ kept stirring at 60 °C for 5 min on a hot plate. After that 5 ml of *Bixa orellana* seed extract was added dropwise in the mixture. Further, the same solution was kept on the magnetic stirrer for 5, 13, and 20 min at 500 rpm as per batches given by factorial design (supplementary table). Using a clean muslin cloth as a filter, the extract was collected.

Before the preparation of nanoparticles, the filtrate was then once more filtered through Whatman filter paper and kept at 4 °C. The transition from bright orange to dark orange confirmed the production of $AgNO_3$ (Aljohar et al., 2022).

2.3.1. Preparation of nano gel

The gel of the prepared BOAgNPs was formulated by adding a gel-forming agent, namely hydroxyl propyl methyl cellulose (HPMC) K15 and Carbopol 940, which was soaked in hot water for 24 h. Subsequently, the BOAgNPs were added to the solution while ensuring uniform stirring through the utilization of a high-speed homogenizer operating at speeds ranging from 7000 to 10,000 revolutions per minute. The pH of the solution was modified to 7.0 by employing triethanolamine as a means to create the gel (Baskar et al., 2018). The resulting gel, involving BOAgNPs, was thereafter kept at ambient temperature. Table 1 presents a summary of the excipients utilized in the formulation.

2.3.2. Characterization of the formulation (Amna et al., 2021; Gur et al., 2022)

2.3.2.1. FTIR spectroscopy. The precise function of the plant extract was verified by fourier transform infrared (FTIR) analysis, which was shepherded to determine the existence of specific purposeful groups and key components. A compatibility analysis of BOAgNPs was undertaken to assess the variation in the graph concerning the functional group.

2.3.2.2. SEM of BOAgNPs. The SEM analysis of the prepared BOAgNPs was conducted using the JSM 6360 instrument manufactured by JEOL India Pvt. Ltd. This analysis aimed to investigate the morphological features and dimensions of the optimized batch of Ag NPs.

2.3.2.3. Appearance and homogeneity. The prepared gel was visually examined for non-quantitative tests like clarity, color, etc. The nanogels that were produced were assessed for homogeneity using a visual examination after placing them in the container. The samples underwent examination to assess the visual characteristics and existence of aggregation.

2.3.2.4. Particle size and polydispersity index. The analysis of size was conducted in the aqueous phase, taking into account the hydration effect, which is reflected in the Z value. The PDI, which is a dimensionless parameter, is utilized to quantify the polydispersity of the formulation. All readings were carried out by the HORIBA SZ 100 analyzer.

2.3.2.5. Compatibility study. FTIR spectrum of BOAgNPs with Carbapol 940 and HPMC K15 was assessed to find evidence of a precise interaction among the drugs and polymer using a Bruker-Aplha II spectrophotometer. A compatibility analysis of BOAgNPs was undertaken to assess the variation in the graph concerning the functional group.

2.3.2.6. pH measurement and drug content. The pH of the nan**o**gel preparation was measured by a pH analyzer. To carry out this determination, a mass of 1 g of nanogel was measured and then dissolved in 10 ml H_2O. The sample was allowed to incubate for a duration of 4–5 min to obtain the correct readings of pH. The data collection process involved obtaining three separate readings.

Drug content was obtained by solubilizing nanogel in 10 ml of ethanol. The combination underwent centrifugation at a speed of 448 relative centrifugal force (RCF) for a duration of 1 h. The liquid supernatant was extracted, and subsequent analysis was conducted on the samples utilizing a UV spectrophotometer at 452 nm wavelength.

Table 2
Protocol of *in-vivo* anticancer study.

Number	Task	Days
1.	To Accumulate and remove hair and left untreated	02
2.	Induction Experiment	Maximum 06 weeks
3.	Treatment Experiment	Maximum 04 weeks
Total Days		10 **weeks**

2.4. In-vitro anticancer cell line study

2.4.1. Cancer cell line procurement and handling

The B16-F10 mouse skin melanoma cell line was incubated in RPMI 1640 media accompanied with 2 mM L-glutamine and 10 % fetal bovine serum. After being seeded into 96-well microtiter plates with 5000 chambers per well and 100 µL of medium, the cells were cultured for a full day. The microtiter plates were inoculated with cells and then cultured for 24 h at 95 % air, 37 °C, 5 % CO_2, and 100 % relative dampness beforehand the investigational medications were added (Je et al., 2022).

2.4.2. Procedure

The chambers were incubated in culture media at a density of 1 × 104 cells/ml for 24 h at 5 % CO_2 and 37 °C. They were seeded at varying concentrations of 20, 40, 60, 80, and 100 µg/ml of samples. The cell line and DMSO (0.2 % in PBS) were incubated in control wells. Every sample endured 3 rounds of incubation.

In a CO_2 incubator, cultured cells were cultured for 24 h at 37 °C and 5 % CO_2. The culturing medium was withdrawn after growth, and 20 µl of MTT reagent (5 mg/min PBS) was supplemented. The treated cells were cultured in a CO_2 incubator for 4 h at 37 °C following the injection of MTT. The formazan crystal growth in the wells was observed under a microscope. Solitary living cells were able to change the yellowish MTT to a dark-colored formazan.

Following the full removal of the medium, 200 µl of DMSO was added and incubated at 37 °C (covered in aluminum foil) and allowed to stand for 10 min. The microplate reader was set to measure absorbance at 550 nm. All observations of the samples were recorded in triplicate.

2.5. In-vivo animal study

2.5.1. Animals

In the investigation, 20–25 g Swiss albino mice, both gender (three males and three females), two months of age, were employed. The inbred mouse colonies were acquired (Regd. No. 1090/PO/Re/S/07/CPCSEA) from Tatyasaheb Kore College of Pharmacy Warananagar, Tal-Panhala Dist-Kolhapur 416113. They were acclimated to 12-hour light–dark cycles, 30–70 % humidity, and a temperature of 23 ± 2 °C. The animals were kept in sterile polypropylene cages with sterile rice husk bedding, and they were randomly assigned to experimental and control groups. Animals received unlimited access to water and ordinary pellets like basal diet. The Tatyasaheb Kore College of Pharmacy at SET in Warananagar, India, has an Institutional Animal Ethical Committee (IAEC) that authorized all of the experiments that were undertaken (REG.No.TKCP/08/23/07). in accordance with the criteria established by the Indian Government's Committee for Control and Supervision of Experiments in Animals (CPCSEA).

2.5.2. Study design

The animals were split up into the following four groups, each consisting of six mice:

- Group I (normal group) had no chemical treatment and was maintained in its usual state.
- For a duration of six weeks, Group II (the Negative Control group) was topically treated with 7,12-dimethylbenz (a) anthracene

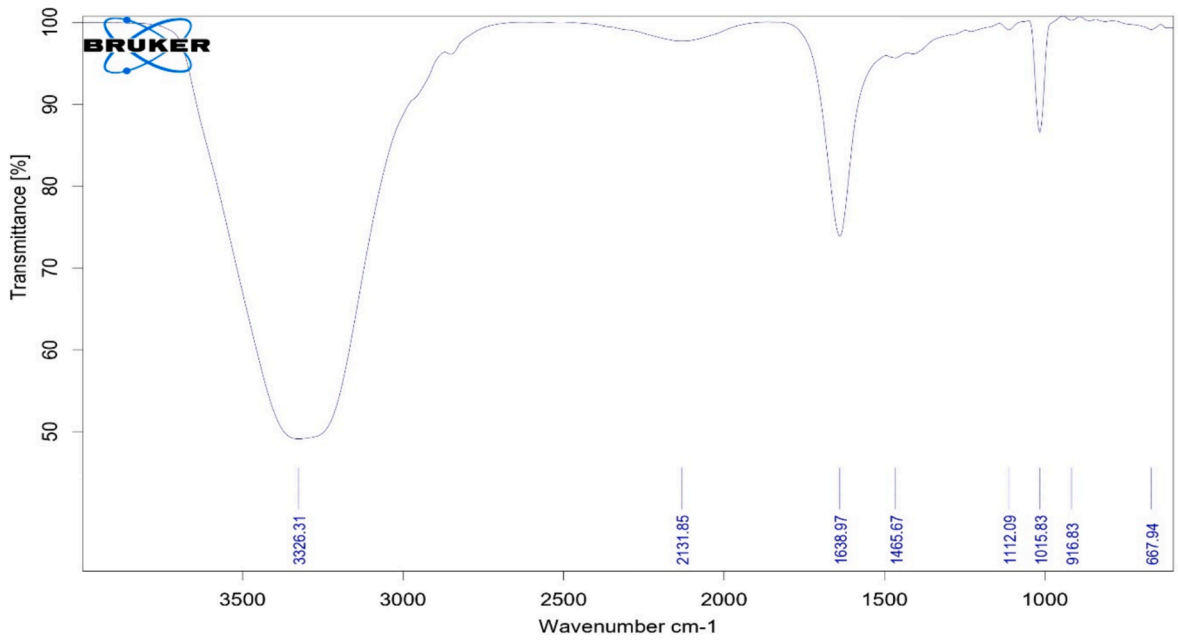

Fig. 1. FTIR Spectrum of BOAgNPs.

(DMBA) without receiving the topical gel that had been produced as a post-treatment.

- Following a 6-week induction phase with DMBA, Group III (the test group) was administered a topical gel loaded with methanolic seed extract.
- The topical gel used in Group IV (the Placebo Group) was blank and devoid of methanolic root extract.

The following table provides a summary of the study's protocol (Table 2).

2.5.3. Procedure

The mice were given depilatory cream to remove all hair from their dorsal region, and then they were left without treatment for 48 h. Following that, mice devoid of hair growth were designated for the in vivo study. The carcinogen 7,12-dimethylbenz (a) anthracene (DMBA) was then injected twice a week for six weeks at a dose of 25 mg/kg in 0.1 mL of acetone per mouse, targeting the hairless dorsal area of the animals (Li and Brakebusch, 2021).

Following a 6-week induction duration, the dorsal regions of the mice were subjected to ocular inspection to identify symptoms resembling skin cancer. The dorsal area of the animal was chosen since it provides more surface area and least disturbed from animal movements (Esteves et al., 2021). Additionally, histological confirmation was performed to validate the presence of these symptoms. The animals were subsequently subjected to a four-week treatment regimen involving the administration of the newly formulated methanolic extract bixin, which contained Ag NPs loaded with nanogel.

According to Singh et al. (2023), the medication was given to the mice once a day at a concentration of 20 g/kg body weight using the

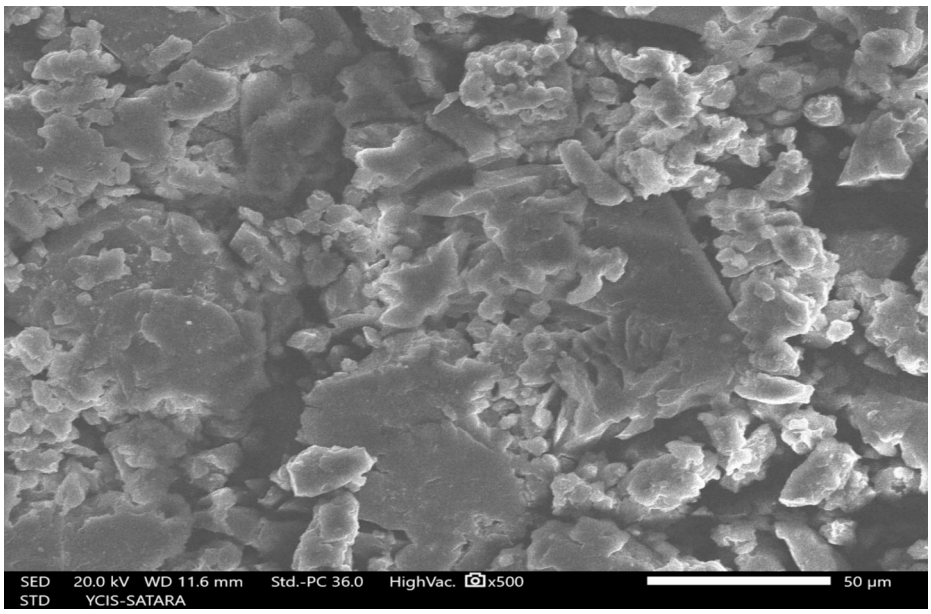

Fig. 2. Scanning Electron Microcopy of BOAgNPs.

Table 3
Particle size and PDI of Nanogel batches.

Run/Batch	Particle size (nm)	Polydispersity index
F1	88.5 ± 1.22	0.401 ± 0.024
F2	88.0 ± 2.31	0.412 ± 0.002
F3	87.6 ± 1.44	0.435 ± 0.013
F4	89.2 ± 0.12	0.425 ± 0.007
F5	93.1 ± 0.31	0.405 ± 0.006
F6	86.5 ± 2.48	0.418 ± 0.008

previously mentioned experimental design. The animals were put to sleep with a large dosage of ether when the treatment phase was over. The topical gel bixin extract's efficacy in treating mice's skin cancer was then evaluated.

The gross morphological changes were recorded and after the treatment protocol, animals were euthanized and the skin was subjected to histological studies. Mice with and without induction were compared for histological skin alterations as part of the study. This was achieved through the application of hematoxylin and eosin stains on paraffin sections from each group. Microscopical evaluation was conducted to determine the increase, decrease, or absence of cancer lesions (Alyoussef and Taha, 2019).

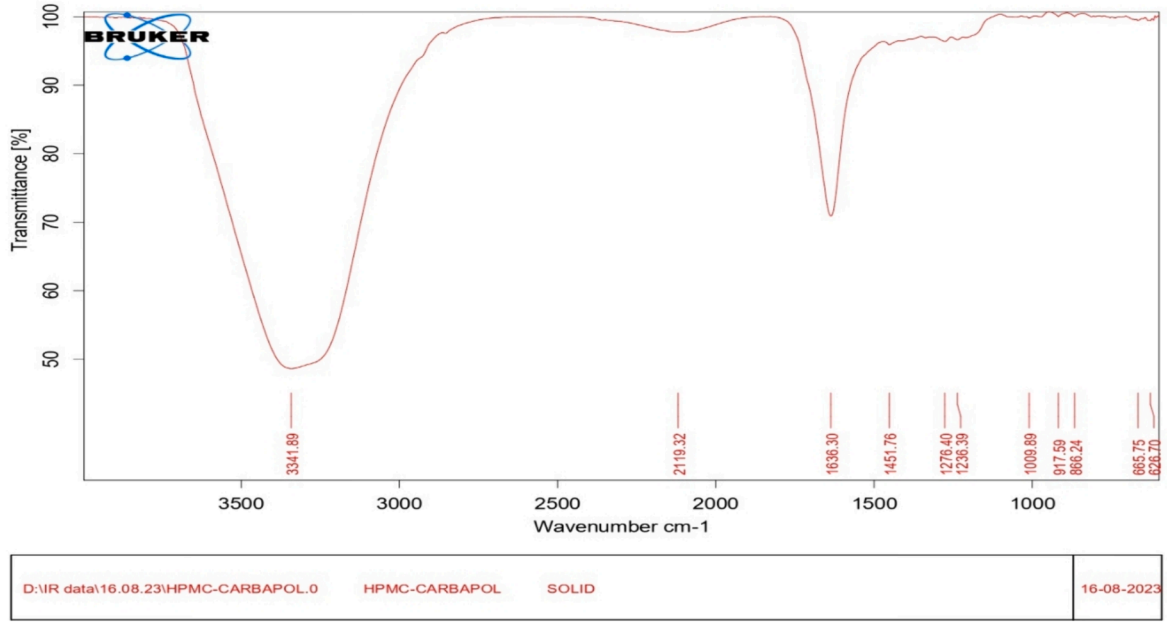

Fig. 3. IR spectrum of Bixin BOAgNPs with carbapol 940.

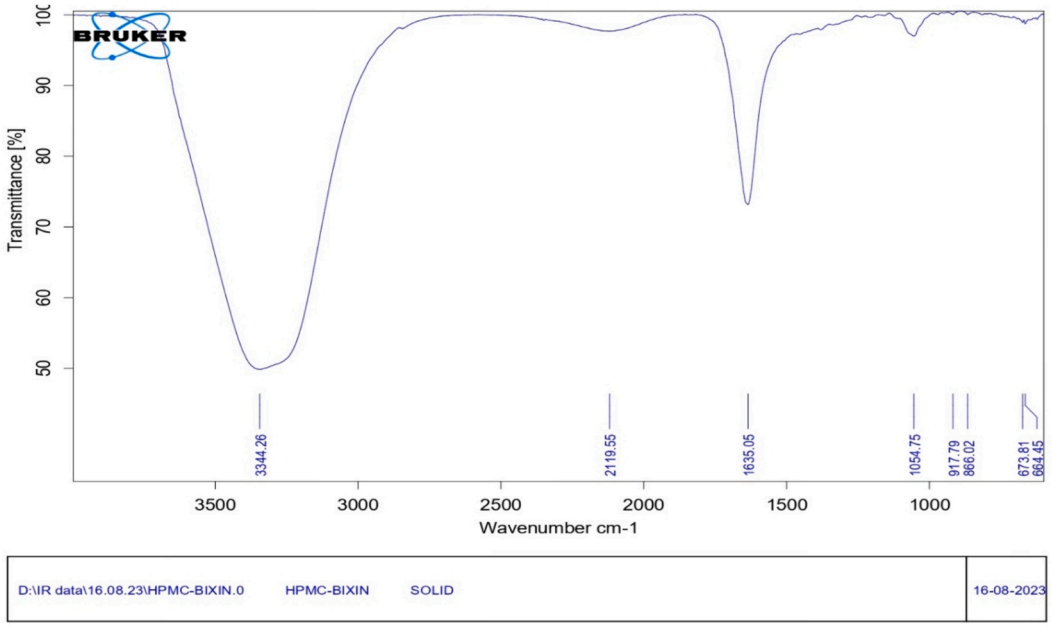

Fig. 4. IR spectrum of Bixin BOAgNPs with HPMC K15.

Table 4
Result of drug content and pH for all formulation batches.

Batch/Formulation	Drug Content (%) (mg gel)	pH
F1	82.30 (±0.28)	6.45 (±0.08)
F2	78.54 (±0.25)	6.51 (±0.05)
F3	71.30 (±0.63)	6.95 (±0.03)
F4	88.74 (±0.14)	6.48 (±0.04)
F5	92.43 (±0.32)	7.10 (±0.02)
F6	90.10 (±0.48)	6.51 (±0.08)

3. Result

3.1. Characterization of BOAgNPs

3.1.1. FTIR spectra of BOAgNPs

The observations from FTIR spectrum analysis indicated peaks at 3326, 1638, and 1465 cm^{-1}. Further, stretching was observed at 1112 cm^{-1}, and bending vibrations at 1015 cm^{-1}. Besides, the spectra indicated no peaks between the ranges of 3000 – 2000 cm^{-1}.

3.1.2. SEM of BOAgNPs

Scanning electron microscopy (SEM) was utilized to witness the characteristics of the particles in nanogel formulation. The analysis suggested that the particles are globular in shape and the typical atom size was obtained to be in the array of 50 μm to 110 μm (Fig. 2).

3.1.3. Evaluation of nano gel

The nanogel was evaluated by its appearance, particle size, and polydispersity index. Six formulations (F1 to F6) prepared by nanogel technology were found to appear clear orange color. These formulations were homogenous and were free from grittiness. The nanoparticle size was analyzed by using a HORIBA SZ-100 analyzer. The observation recorded for particle size and polydispersity index is represented in Table 3. The highest particle size was observed for the F5 formulation (93.1 nm) and the lowest was for the F6 formulation (86.5 nm). Besides, the polydispersity index for the different formulations was found to be between the range 0.401 (F1 formulation) and 0.435 (F3 formulation).

3.1.4. Polymers compatibility study by FTIR

Compatibility studies of BOAgNPs were conducted with two polymers like, Cabapol 940 (Fig. 3) and HPMC K-15 (Fig. 4). The IR spectra of Carbapol 940 with BOAgNPs of the spectrum indicated stretching vibrations at 3341, 1636, 1451, and 1230 cm^{-1}. Further, the IR spectrum of BOAgNPs with HPMC K-15 indicated three stretching vibrations such as at 3344, 1635, and 1054 cm^{-1}.

3.1.5. Drug content and pH measurement

The pH measurement of different formulations ranged between 6.45 (F1 formulation) and 7.10 (F5 formulation). The highest drug content was observed in the F5 formulation (92.43 %) while the lowest was seen in the F3 formulation (71.30 %) (Table 4).

3.2. In-vitro anticancer cell line study

The formulation that had the maximum drug content (F5 code named as E1) was used for the in-vitro anticancer activity. Five dissimilar concentrations such as 20, 40, 60, 80, and 100 μg/ml were tested on the cancer cell lines B16F10. The effects were compared with a standard drug, 5-Flurouracil. The concentration-dependent activity such as percentage inhibition and percentage viability observed with the test compounds is represented in Table 4. Both standard as well as E1 exhibited a concentration-dependent activity and the highest inhibition was observed at 100 μg/ml (78.72 % for 5-Flurouracil and 45.67 % for

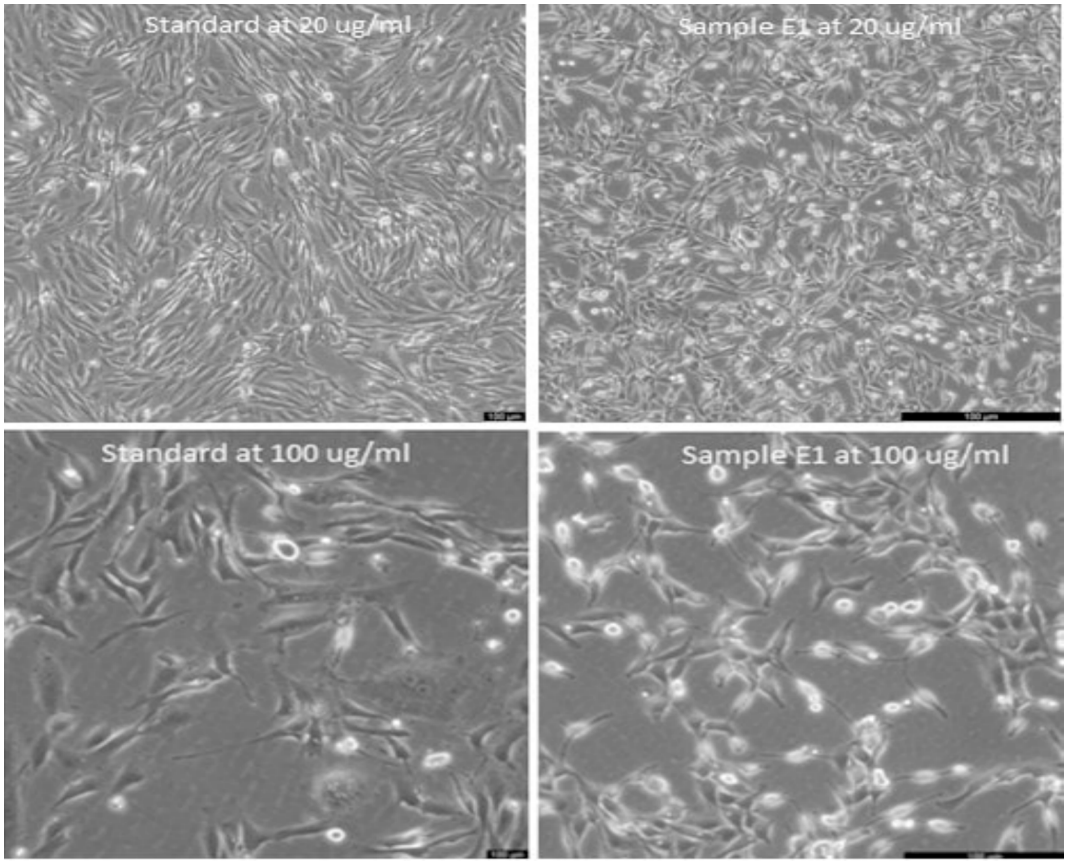

Fig. 5. Microscopic results for anticancer cell line study.

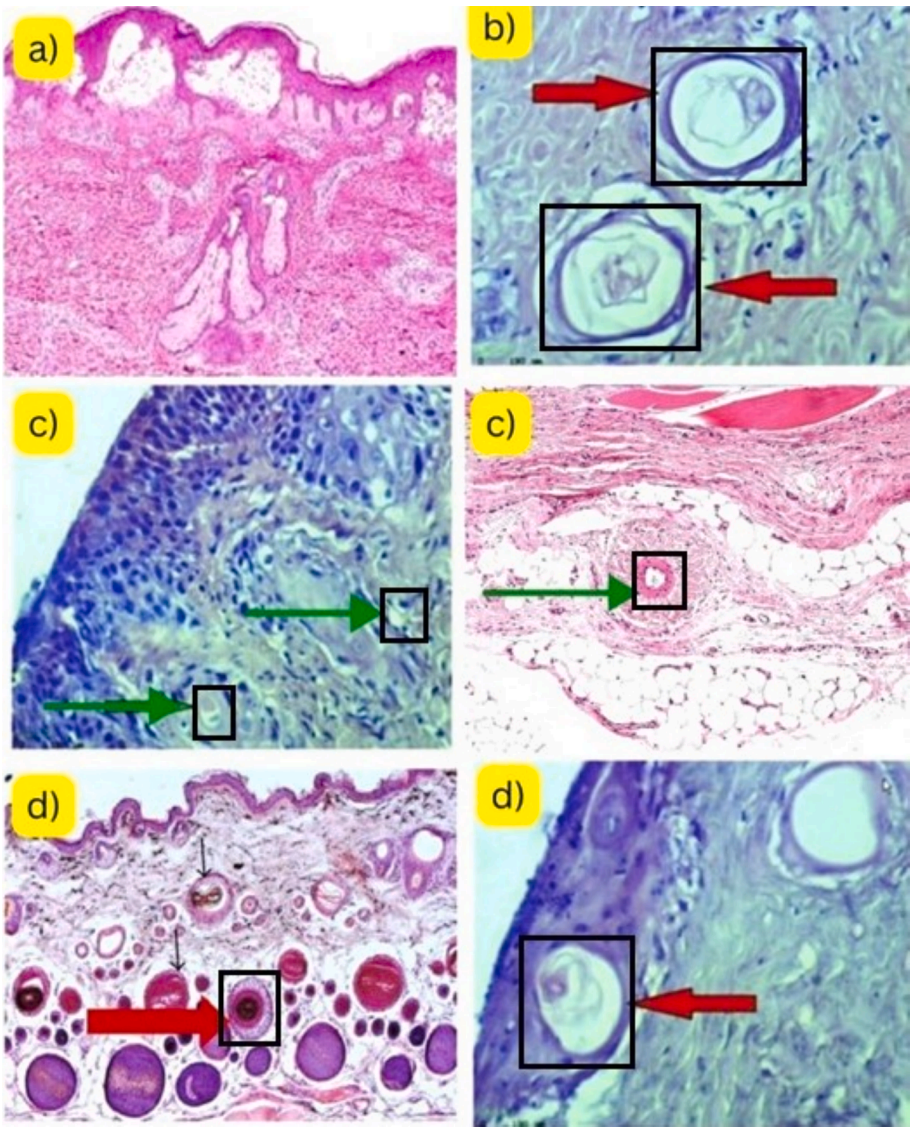

Fig. 6. Effect of BOAgNP on skin histology. Fig. 6a. Histological examinations revealed the existence of huge keratinocyte pearls.Fig. 6b. Histological illustration of keratinocyte pearl formation of squamous cell carcinoma. Fig. 6c. Histological illustration of skin tissue mending naturally, reduced size of skin keratinocyte pearl. Fig. 6d, histological illustration of skin tissue in unchanged pattern of keratinocyte pearls.

E1). Since the inhibitory effect with E1 did not cross 50 % when the maximum dose was tested, the IC_{50} value was calculated only for the standard drug and was found to be 38.25 μg/ml. The microscopic observation and result for the percentage inhibition as well as viability when the lowest dose (20 μg/ml) and highest dose (100 μg/ml) are indicated in Fig. 5.

3.3. *In-vivo anticancer study*

Group I, the control group, showed skin tissue with a histological pattern within a normal range. The epidermis tissue of the non-treated (control) group has a consistent organization of epidermal cell layers with an underlying dermal layer, as revealed in Fig. 6a. Histological examinations in Group II revealed the existence of huge keratinocyte pearls, as seen in Fig. 6b. An illustration of keratinocyte pearl formation in squamous cell cancer is shown in Fig. 6b.

Tissue observations of the skin in mice treated topically with gel after skin cancer growth are shown in Fig. 6c (Group III). The picture on the slide illustrates the phenomenon of skin tissue mending naturally, as shown by the shrinkage of the skin keratinocyte pearl and highlighted by green arrows. The slide observation investigations showed that there was no discernible difference between Group II and Group IV. As seen in Fig. 6d, the skin tissue of the animals in the final group (Group IV) displayed an unchanged pattern of keratinocyte pearls, suggesting that the therapy was unsuccessful.

Fig. 7 depicts the visual examination conducted during the treatment phase, which spanned duration of four weeks, utilizing the topical gel. The mice belonging to group I (as depicted in Fig. 7a) exhibited skin that appeared to be within the normal array, in contrast to the skin of the control group II (negative, as shown in Fig. 7b). The mice belonging to group III (as depicted in Fig. 7c) showed a significantly enhanced level of skin healing in comparison to the mice in group IV (as illustrated in Fig. 7d).

4. Discussion

In the present study, a nanogel formulation of bixin was evaluated for anticancer activity. A green synthesis method was approved for the silver nanoparticle formulation of bixin seed extract. Characterization of the formulation revealed the existence of important purposeful groups typically identified in the extract. The nano gel formulation exhibited a moderate inhibitory effect against B16F10 cancer cell lines. However,

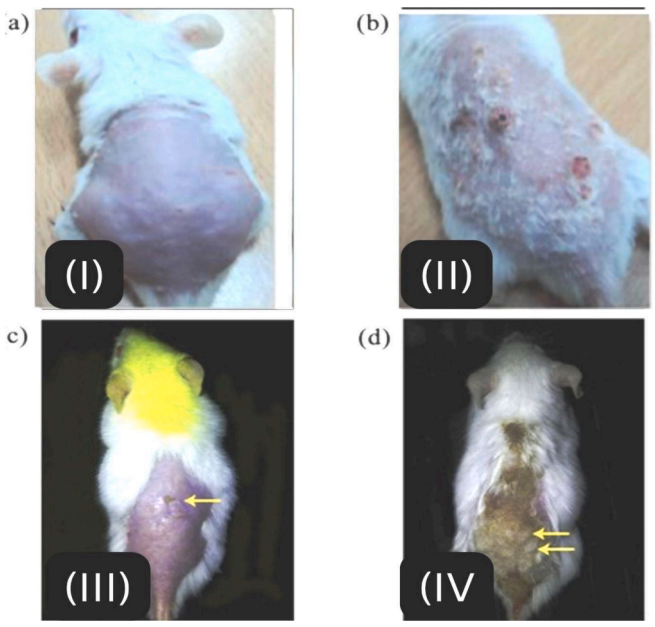

Fig. 7. Macroscopical characteristics of skin after treatment with BOAgNP.

when a study was conducted on animals, a promising anticancer activity, as well as a healing effect, was observed with the bixin-nano gel formulation (Table 3 to 5 and Figs. 1 to 7).

In this method, the bixin was isolated from the seeds of *B.orellana* and while doing so all the precautions indicated the literature were followed to maintain the integrity of the active component (Carballo-Uicab et al., 2019). Some of the important measures adopted include maintaining rigid control over temperature and pressure as well as the duration of the extraction process. All these parameters are reported to be essential for preserving the integrity of the active component, bixin (Xu and Kong, 2017). During new product development, the biggest task is to make a formulation that maintains the stability and integrity of the active pharmaceutical ingredient. This process becomes more complicated while formulating an active ingredient isolated from a plant source (Matalqah et al., 2020). Due to such drawbacks, the fundamental concept underlying the integration of innovative medication delivery techniques in herbal medicines is being extensively investigated in the literature. The integration of innovative drug delivery systems and traditional diseased healing remedies holds significant importance in addressing the challenges posed by progressively severe diseases (Khizar et al., 2023). Historically, herbal medicines were not prioritized for the creation of new formulations due to the absence of scientific rationale and challenges associated with processing, including standardization, extraction, and identification of specific medicinal components within intricate polyherbal systems (Qiu et al., 2022; Matalqah et al., 2020).

The characterization readings of the green production of the bixin suggested FTIR spectra peaks at 3326, 1638, and 1465 cm^{-1}. According to previous studies, these peaks are indicative of the existence of active groups such as O–H. C–H and C = C. Further, stretching perceived at 1112 cm^{-1}, suggested the occurrence of C-O in the compound. And, bending vibrations observed at 1015 cm^{-1} are reported to be due to the C–H functional group in the test compound of the formulation (Amna et al., 2021). Studies also suggested that the absence of any peak between 3000 – 2000 cm^{-1} suggested that functional groups might have played a role of reducing agents in converting Ag + to AgO (Mughees and Wajid, 2021). Such types of characteristic features might work as a stabilizing agent during the synthesis of silver nanoparticles (Miu and Dinischiotu, 2022).

The SEM analysis in the current study revealed that the particle size is a spherical shape. Such types of particles according to previous studies give a smooth texture to the formulation (Amna et al., 2021). Besides,

Table 5
Effects of test samples against B16F10 Cancer cell line.

Sl. no.	Sample code	Conc. (µg/ml)	OD			Mean	% Inhibition	% Viability	IC_{50} (µg/ml)
1	Control		1.307			–	–	–	–
2	Standard	20	0.739	0.739	0.739	**0.739**	**43.45**	**56.54**	**38.25**
		40	0.628	0.628	0.628	**0.628**	**51.95**	**48.04**	
	(5-FU)	60	0.551	0.550	0.551	**0.550**	**57.91**	**42.08**	
		80	0.436	0.436	0.437	**0.436**	**66.64**	**33.35**	
		100	0.279	0.278	0.279	**0.278**	**78.72**	**21.27**	
3	E1	20	1.008	1.006	1.008	**1.007**	**22.95**	**77.04**	**NE**
		40	0.901	0.902	0.901	**0.901**	**31.06**	**68.93**	
	(F5)	60	0.824	0.825	0.824	**0.824**	**36.95**	**63.04**	
		80	0.782	0.784	0.782	**0.782**	**40.16**	**59.83**	
		100	0.710	0.712	0.710	**0.710**	**45.67**	**54.32**	

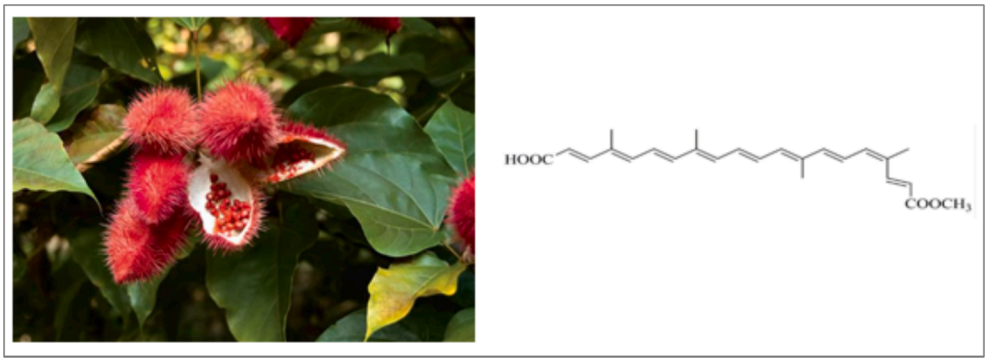

Fig. 8. The .
Source and structure of bixin (Xu and Kong, 2017; Shanmuganathan et al., 2019)

the particle size in the range of 50 – 110 μm was reported to be ideal for a drug molecule to achieve its intended therapeutic activity (Das et al., 2022). The analysis from the HORIBA SZ-100 analyzer suggested that the size of nanoparticles in all the formulations was around 88 nm and the polydispersity index was 0.416. According to previous studies, these values suggest the optimum characteristics needed for the nanogel particles during the new formulation development process (Gur et al., 2022).

The IR spectral analysis of BOAgNPs with Carbapol 940 confirmed the occurrence of active groups such as O–H (stretching at 3341 cm^{-1}), C = C (stretching at 1636 cm^{-1}), C–H (stretching at 1451 cm^{-1}) and C-O (stretching at 1230 cm^{-1}) (Amna et al., 2021). The observations suggested that mixing BOAgNPs with polymer (Carbapol 940) did not produce any chemical change. Earlier studies have indicated that Carbapol 940 is a compatible polymer and does not normally show interactions with medications in the formulation development process (Nawaz et al., 2022). The source as well as the structure of bixin is represented in Fig. 8.

Additionally, the IR spectra analysis of BOAgNPs with HPMC K-15 also confirmed the presence of O–H (stretching at 3344 cm^{-1}), C = C (stretching at 1635 cm^{-1}), and C-O (stretching at 1054 cm^{-1}). These were suggestive of the incidence of useful groups in the compound and no chemical change or interactions might have occurred with HPMC K-15. The polymer in the earlier study has been routinely used for the preparation of various formulations due to compatibility and non-interacting characteristics (Li et al., 2021). Furthermore, the pH of different formulations was found to be around 6.66. This value according to the literature is optimum for a formulation to avoid incidences of irritation when the drug is administered (Amna et al., 2021). Further, the average drug amount in the formulation was estimated to be 83.9 %. This value is by previous research that reports the desired efficacy needed for a formulation (Gur et al., 2022).

From the current study's data, it was found that formulation E1 (code-named for F5) has moderately reduced the viability of B16F10 in comparison with the standard. By the cytotoxic studies, E1 at 20 ug/ml has yielded 77.04 % viability and 22.95 % inhibition, which is a moderate result as compared to standard. Simultaneously, for 100 ug/ml, it showed 54.32 % viability and 45.67 % inhibition. The result of *in-vitro* anti-cancer activity revealed that on cell line B16F10, the formulation showed nearly 60 % inhibition when compared to the standard (5-Flurouracil). The resultant percentage of inhibition can be increased if the concentration of drug bixin in the manager is proportionately increased in the formulation. Such types of inhibitory anticancer activity depending on the concentration of the drug can be found in the previous work (Je et al., 2022; Kim et al., 2023).

The *in-vivo* anticancer activity indicated a suppression in the tumorogenic activity induced by a chemical carcinogenic agent (DMBA) when bixin nanogel formulation was applied to the skin of mice. The chemical carcinogen (DMBA) is reported to cause DNA adducts, and promote growth by modulating gene expression leading to tumor progression (Ashraf et al., 2023). The formulation was found to effectively inhibit the changes such as keratinocytes pearl formation and squamous cell carcinoma, when compared with placebo gel treatment. Similarly, the macroscopical observations suggested that bixin nanoparticle gel prevented cancer formation on the skin. Moreover, the treatment of bixin gel appears to initiate the healing process, when the observations were compared with the placebo gel-treated group. The studies conducted in the past suggested that bixin exhibits anticancer activity by multiple pathways such as cell cycle inhibition, induction of apoptosis in cancerous cells through inhibition of COX-1 as well as COX-2 enzymes and growth inhibition in the cancerous cells (Ashraf et al., 2023).

In the current study, a unique approach to the preparation of a silver nanoparticle gel formulation of bixin was effectively tried. The use of nanoparticle technology is widespread in many domains, including medicine formulation. According to reports, this method works with a variety of chemicals, including gels, copolymers, colloids, organic, and inorganic (Mughees and Wajid, 2021). Since it is possible to efficiently overcome the issues related to phytochemical formulation, the green production of nanoparticles is becoming more and more popular. In addition to being environmentally benign, this technology is said to be non-toxic, economical, and to provide the active components with better stability properties (Miu and Dinischiotu, 2022).

In contrast to alternative methods, the nano-particle formulation managed to maintain the active ingredient quality and seems to have administered the medication at the intended location as efficiently as possible (Shanmuganathan et al., 2019). According to the information that is currently accessible in the literature, green nanoparticle production has a number of uses in the biomedical area, including immunological, regenerative, tissue repair, diagnostics, wound healing, and biosensing (Mughees and Wajid, 2021; Miu and Dinischiotu, 2022). The findings of the present study indicated a promising anticancer property of bixin in nanoparticle gel formulation, however, more research is essential to establish its pharmacokinetic as well as pharmacodynamic profile before establishing its therapeutic potential.

5. Conclusion

According to the discoveries of this study, the silver nanoparticle formulation of bixin seed extract showed anticancer activity. Optimum drug content, pH, and characterization of bixin suggested that the silver nanoparticle gel formulation did not changed drastically and might be a promising option for target delivery of phytochemicals such as bixin. The easy technique of formulation and bixin being a plant derivative might enhance affordability and reduce the economic burden of the disease. More research conducted in this direction could identify a safe and efficacious topical formulation for treating skin cancers.

Funding

The authors would like to express gratitude to King Saud University, Riyadh, Saudi Arabia, for extending financial support to do this research project through the Researchers Supporting Project number (RSP2024R146). The authors are also thankful to AlMaarefa University for supporting this research.

CRediT authorship contribution statement

Swapnil S. Patil: Writing – original draft, Methodology, Investigation, Formal analysis, Conceptualization. **Preeti khulbe: . Manojkumar M. Nitalikar:** Writing – review & editing, Project administration, Methodology, Conceptualization. **Kuntal Das:** Writing – review & editing, Software, Methodology, Data curation. **Mallikarjuna B.P:** Writing – original draft, Validation, Resources, Conceptualization. **Sultan Alshehri:** Writing – review & editing, Software, Investigation, Funding acquisition, Conceptualization. **Amro Mohammed Sawadi Khormi:** Writing – original draft, Formal analysis, Conceptualization. **Mutlaq Eidhah M. Almalki:** Writing – original draft, Resources, Methodology, Conceptualization. **Syed Arif Hussain:** Writing – review & editing, Methodology, Formal analysis, Data curation. **Syed Imam Rabbani:** Writing – review & editing, Visualization, Methodology, Conceptualization. **Syed Mohammed Basheeruddin Asdaq:** Writing – review & editing, Methodology, Conceptualization.

Declaration of competing interest

The authors declare that they have no known competing financial interests or personal relationships that could have appeared to influence the work reported in this paper.

Acknowledgments

The authors would like to acknowledge the Researchers Supporting

Project number (RSP2024R146), King Saud University, Riyadh, Saudi Arabia, for extending financial support to do this research project.

Appendix A. Supplementary material

Supplementary data to this article can be found online at https://doi.org/10.1016/j.jsps.2024.102125.

References

Ahmed, B., Qadir, M.I., Ghafoor, S., 2020. Malignant melanoma: skin cancer-diagnosis, prevention, and treatment. Crit. Rev. Eukaryot. Gene. Expr. 30 (4), 291–297.

Aljohar, A.Y., Muteeb, G., Zia, Q., Siddiqui, S., Aatif, M., Farhan, M., et al., 2022. Anticancer effect of zinc oxide nanoparticles prepared by varying entry time of ion carriers against A431 skin cancer cells *in-vitro*. Front. Chem. 1069450, 1–13.

Alyoussef, A., Taha, M., 2019. Blocking Wnt as a therapeutic target in mice model of skin cancer. Arch. Dermatol. Res. 311 (8), 595–605.

Amna, M.T., Khan, U.N., Amin, B., Javed, M.T., Mehmood, S., Farooq, M.A., et al., 2021. Characterization of bio-fabricated silver nanoparticles for distinct anti-fungal activity against sugarcane phytopathogens. Microsc. Res. Tech. 84 (7), 1522–1530.

Ashraf, A., Ijaz, M.U., Muzammil, S., Nazir, M.M., Zafar, S., Zihad, S.M.N.K., et al., 2023. The role of bixin as antioxidant, anti-inflammatory, anticancer, and skin protecting natural product extracted from *Bixa orellana* L. Fitoterapia. 169, 105612.

Baskar, V., Meeran, S., Shabeer, T.K., Subramani, A., Sruthi, A.J., 2018. Historic review on modern herbal nanogel formulation and delivery methods. Int J Pharm PharmSci 10 (10), 1–10.

Bray, F., Ferlay, J., Soerjomataram, I., Siegel, R.L., Torre, L.A., Jemal, A., 2018. Global cancer statistics 2018: GLOBOCAN estimates of incidence and mortality worldwide for 36 cancers in 185 countries. CA Cancer J. Clin. 68 (6), 394–424.

Carballo-Uicab, V.M., Cárdenas-Conejo, Y., Vallejo-Cardona, A.A., Aguilar-Espinosa, M., Rodríguez-Campos, J., Serrano-Posada, H., Narváez-Zapata, J.A., Vázquez-Flota, F., Rivera-Madrid, R., 2019. Isolation and functional characterization of two dioxygenases putatively involved in bixin biosynthesis in annatto (Bixa orellana L.). PeerJ. 21 (7), e7064.

Coelho, Dos, Santos, D., Silva, B.A.D., Ribeiro, J.S., Rodrigues, Junior, S.A., Campos, Â. D., Lund, R.G. 2022. *Bixa orellana* L. (Achiote, Annatto) as an antimicrobial agent: A scoping review of its efficiency and technological prospecting. J Ethnopharmacol. 287:114961.

Cruz-Martins, N., 2023. Advances in plants-derived bioactives for cancer treatment. Cells. 12 (8), 1112.

Das, P., Manna, S., Behera, A.K., Shee, M., Basak, P., Sharma, A.K., 2022. Current synthesis and characterization techniques for clay-based polymer nano-composites and its biomedical applications: a review. Environ. Res. 212 (Pt E), 113534.

David, S.J., Julián, G.C., Liliana, V.C., Ayala-Aponte, A.A., Liliana, S.C., 2022. Kinetics and bixine extraction time from achiote (*Bixa Orellana* L.). J. FoodSci Technol. 59 (3), 1239–1246.

Dildar, M., Akram, S., Irfan, M., Khan, H.U., Ramzan, M., Mahmood, A.R., et al., 2021. Skin cancer detection: a review using deep learning techniques. Int. J. Environ. Res. Public Health 18 (10), 5479.

Dorrell, D.N., Strowd, L.C., 2019. Skin cancer detection technology. Dermatol. Clin. 37 (4), 527–536.

Esteves, M., Silva, C., Pereira, S.S., Morais, T., Moreira, Â., Costa, M.M., Monteiro, M.P., Duarte, J.A., 2021. Regular voluntary running inhibits androgen-independent prostate cancer growth in mice. J. Phys. Act. Health 18 (6), 653–659.

Gonçalves, A.C., Richiardone, E., Jorge, J., Polónia, B., Xavier, C.P.R., Salaroglio, I.C., 2021. Impact of cancer metabolism on therapy resistance - clinical implications. Drug Resist Updat. 59, 100797.

Gur, T., Meydan, I., Seckin, H., Bekmezci, M., Sen, F., 2022. Green synthesis, characterization and bioactivity of biogenic zinc oxide nanoparticles. Environ. Res. 204, 111897.

Huang, J., Li, J.X., Ma, L.R., Xu, D.H., Wang, P., Li, L.Q., et al., 2022. Traditional herbal medicine: a potential therapeutic approach for adjuvant treatment of non-small cell lung cancer in the future. Integr Cancer Ther. 21, 15347354221144312.

Jarouche, M., Suresh, H., Low, M., Lee, S., Xu, C., Khoo, C., 2019. Quality control and variability assessment of an eight-herb formulation for hypertension using method validation and statistical analysis. Molecules 24 (8), 1520.

Je, J.G., Jiang, Y., Heo, J.H., Li, X., Jeon, Y.J., Ryu, B.M., 2022. Mitigative effects of PFF-a isolated from *ecklonia cava* on pigmentation in a zebrafish model and melanogenesis in B16f10 cells. Mar. Drugs 20 (2), 123.

Khizar, S., Alrushaid, N., Alam, K.F., Zine, N., Jaffrezic-Renault, N., Errachid, A., et al., 2023. Elaissari A. nanocarriers based novel and effective drug delivery system. Int. J. Pharm. 632, 122570.

Kim, J., Lee, N., Chun, Y.S., Lee, S.H., Ku, S.K., 2023. Krill Oil's Protective benefits against ultraviolet B-induced skin photoaging in hairless mice and *In-vitro* Experiments. Mar. Drugs 21 (9), 479.

Li, H., Brakebusch, C., 2021. Analyzing skin tumor development in mice by the DMBA/TPA model. Methods Cell Biol. 163, 113–121.

Li, Z., Sun, Y., Bar-Shalom, D., Mu, H., Larsen, S.W., Jensen, H., et al., 2021. Towards functional characterization of excipients for oral solid dosage forms using UV-vis imaging. liberation, release and dissolution. J. Pharm. Biomed. Anal. 194, 113789.

Matalqah, S.M., Aiedeh, K., Mhaidat, N.M., Alzoubi, K.H., Bustanji, Y., Hamad, I., 2020. Chitosan nanoparticles as a novel drug delivery system: a review article. Curr. Drug. Targets 21 (15), 1613–1624.

Miu, B.A., Dinischiotu, A., 2022. New green approaches in nanoparticles synthesis: an overview. Molecules 27 (19), 6472.

Mughees, M., Wajid, S., 2021. Herbal based polymeric nanoparticles as a therapeutic remedy for breast cancer. Anticancer Agents Med. Chem. 21 (4), 433–444.

Nawaz, A., Latif, M.S., Alnuwaiser, M.A., Ullah, S., Iqbal, M., Alfatama, M., et al., 2022. Synthesis and characterization of chitosan-decorated nanoemulsion gel of 5-fluoro-uracil for topical delivery. Gels. 8 (7), 412.

Panahishokouh, M., Noroozian, M., Mohammadian, F., Khanavi, M., Mirimoghaddam, M., Savar, S.M., et al., 2023. Evaluation of the effectiveness of an herbal formulation of *boswellia sacra flueck*. in improving cognitive and behavioral symptoms in patients with cognitive impairment and alzheimer's disease. J. Res. Pharm. Pract. 11 (3), 91–98.

Panja, A., Mishra, A.K., Dash, M., Pandey, N.K., Singh, S.K., Kumar, B., 2021. Silver nanoparticles – a review. EJMO. 5 (2), 95–102.

Qiu, Z., Yu, Z., Xu, T., Wang, L., Meng, N., Jin, H., et al., 2022. Novel nano-drug delivery system for brain tumor treatment. Cells 11 (23), 3761.

Shadisvaaran, S., Chin, K.Y., Mohd-Said, S., Leong, X.F., 2023. Therapeutic potential of bixin on inflammation: a mini review. Front. Nutr. 10, 1209248.

Shanmuganathan, R., Karuppusamy, I., Saravanan, M., Muthukumar, H., Ponnuchamy, K., Ramkumar, V.S., Pugazhendhi, A., 2019. Synthesis of silver nanoparticles and their biomedical applications - a comprehensive review. Curr. Pharm. Des. 25 (24), 2650–2660.

Singh, S., Sonia, S.R.K., Alsayegh, A.A., Batiha, G.E., Alotaibi, S.S., *et al.* 2023. Formulation development and investigations on therapeutic potential of nanogel from *beta vulgaris* l. extract in testosterone-induced alopecia. Biomed Res Int. 2023: 1777631.

Tao, S., Yang, Y., Li, J., Wang, H., Ma, Y., 2021. Bixin attenuates high-fat diet-caused liver steatosis and inflammatory injury through nrf2/PPAR*A* signals. Oxid. Med. Cell. Longev. 6610124.

Xu, Z., Kong, X.Q., 2017. Bixin ameliorates high fat diet-induced cardiac injury in mice through inflammation and oxidative stress suppression. Biomed. Pharmacother. 89, 991–1004.

Youn, B.Y., Kim, J.H., Jo, Y.K., Yoon, S., Im, J.Y., Kim, H.J., et al., 2023. Current characteristics of herbal medicine interventions for cancer on clinical databases: a cross-sectional study. Integr. Cancer Ther. 22, 15347354231218255.